JOURNAL OF MATERIALS SCIENCE 19 (1984) 1818–1826

Effect of irradiation particle mass on crystallization of amorphous alloys

J. L. BRIMHALL
Pacific Northwest Laboratory, Richland, Washington 99352, USA

The crystallization temperature of amorphous alloys was found to be significantly lowered by heavy ion or electron irradiation during annealing. However, only heavy ion irradiation altered the mode of crystallization. Both a binary and multi-element amorphous alloy showed this type of response to irradiation. Radiation-enhanced diffusion processes in the amorphous state can explain the increased crystallization kinetics during irradiation. Heavy ion irradiation alters the crystallization mode by causing direct transformation to the final equilibrium phase as opposed to intermediate metastable phase formation during thermal annealing or electron irradiation. The equilibrium phase is believed to nucleate directly in the displacement cascades, which only form during heavy ion bombardment.

1. Introduction

Electron and heavy ion irradiation produce different point defect distributions and hence different damage states in crystalline material. Electron irradiation damage is relatively uniform, whereas heavy ion irradiation damage is highly localized in displacement cascades. It is postulated that similar differences occur in defect distributions in heavy ion and electron irradiated amorphous materials. Atomic mobility is, therefore, affected in amorphous as well as crystalline material by the creation of excess point defect concentration. Hence, differences in the damage states in amorphous alloys created by electrons as opposed to ion irradiation should be manifested by observed changes in the rates and mode of crystallization.

In previously published work, we have shown that heavy ion irradiation alters both the kinetics and mode of crystallization in an amorphous alloy [1, 2]. A detailed study of a complex, amorphous Fe–Cr–Ni–W alloy showed the crystallization temperature (T_c) to be 100 to 150 K lower during ion irradiaton. Furthermore, a χ-phase formed directly from the amorphous phase during ion irradiation, whereas a two-phase structure, α-iron solid solution plus χ-phase, formed during thermal annealing [1]. Other work has generally shown a lowering of T_c during ion or electron irradiation although there have been ambiguous results [3–7]. Irradiation-induced changes in crystallization mode have not been widely studied.

In the work reported here, the influence of heavy ion irradiation on the kinetics and mode of crystallization of a simple amorphous MoNi alloy has been studied. In addition, both the amorphous MoNi and the previously studied amorphous Fe–Cr–Ni–W alloy have been electron irradiated in a voltage electron microscope (HVEM). All of the microstructural changes were characterized by transmission electron microscopy (TEM) following the various irradiation treatments.

These results as well as the previous results are utilized to arrive at a more complete description of the effect of irradiation on crystallization behaviour. The ion and electron irradiation results are compared to determine the specific role of the bombarding particle in altering the mode of crystallization. The use of both a simple binary amorphous alloy and a multi-element alloy gives more general applicability to the results. All the results are discussed in terms of radiation-enhanced diffusion processes and the effects of high energy displacement cascades.

2. Experimental procedure

Both the MoNi and Fe–Cr–Ni–W amorphous

0022–2461/84 $03.00 + .12

alloys were porduced using high-rate sputter deposition on to a cold substrate. The sputtered films, 0.25 mm thick, were cut into 3 mm sections for subsequent irradiation. The thermal annealing behaviour of these particular amorphous alloys has been reported previously [1, 8].

Specimens of MoNi were irradiated with 5 MeV Ni^{2+} ions at a dose rate of $\sim 5 \times 10^{12}$ ions cm^{-2} sec^{-1}. This produced a displacement rate of $\sim 4 \times 10^{-3}$ displacements per atom sec^{-1} at a distance of 0.5 μm from the surface. These same conditions had been used for the Fe–Cr–Ni–W alloy [1]. The dose range extended from 0.2 to 20 displacements per atom, and irradiation temperatures varied from $\leqslant$ 500 to 960 K for the MoNi alloy.

Additional specimens of the amorphous alloys were irradiated with 1.2 or 1.5 MeV electrons in the HVEM at Lawrence Berkeley Laboratory. Specimens were heated to a temperauture considerably below T_c and irradiated for 15 to 30 min. The temperature was increased in 25 K intervals and held for 15 to 30 min at each temperature until crystallization occurred. Displacement cross-sections varied between 28 and 35 barn for the MoNi alloy and 40 to 40 barn for the Fe–Cr–Ni–W alloy for this electron energy range. The calculated displacement rate was in the range 2 to 3×10^{-3} displacements per atom sec^{-1}.

All microstructural analysis utilized TEM. The ion bombardment specimens were electropolished such that a region 0.5 μm from the surface was observed in the electron microscope. The damage zone extended to ~ 1.5 μm, so some specimens were thinned completely through the damage zone to confirm that the observed effects were due to the irradiation. The electron-irradiated specimens were examined directly in the HVEM.

3. Results

Both concurrent ion or electron irradiation and annealing reduced T_c in amorphous MoNi and Fe–Cr–Ni–W alloys. Ion irradiation had a greater effect than electron irradiation. Ion irradiation also promoted direct transformation of the amorphous phase to an equilibrium crystal phase as opposed to intermediate metastable phase transitions caused by thermal annealing without irradiation. The crystallization mode caused by electron irradiation was similar to that caused by thermal annealing but was different than that caused by ion irradiation.

3.1. Heavy ion irradiation

Heavy ion irradiation of amorphous MoNi at elevated temperatures produced an ultra-fine grained, uniform microstructure as illustrated in Fig. 1. A temperature of 830 K was the lowest temperature at which this grain structure was resolvable. The change in microstructure was accompanied by a sharpening of the diffuse diffraction rings. With increasing dose, the crystallites became larger and more clearly resolved (Figs. 1b and c), and the diffraction rings also continually sharpened and new rings appeared.

The influence of irradiation on the crystallization kinetics is shown on a time–temperature–transformation (TTT) diagram (Fig. 2) which delineates the transformation as a function of time and temperature. The distinction between an amorphous and crystalline structure was determined by the appearance of spottiness in a micro-diffraction pattern taken from a very small area (Fig. 3). Resolution of small crystal in dark-field micrographs was also used (Figs. 4a and b). For crystals < 4 nm diameter, it was a somewhat subjective interpretation as to whether the matrix was crystalline or not. As-deposited, amorphous structure can also show a certain degree of spottiness. Fig. 2, however, shows an approximation of the irradiation times and temperatures that separate amorphous and crystalline structures. Crystallization without irradiation was clearly distinguishable, and it is clear from Fig. 2 that there was accelerated crystallization during irradiation with heavy ions. This observation is in complete agreement with the previous results of ion irradiation of the Fe–Cr–Ni–W amorphous alloy [1].

The slope of the curve separating the crystalline and amorphous regions in Fig. 2 suggests that 700 to 770 K is a critical temperature region. Material irradiated below 770 K would require an extremely long time, but specimens irradiated at 830 K crystallized in a very short time. Of two specimens irradiated to a high dose at 770 K, one crystallized and the other did not. Inaccuracy in temperature measurements could produce an actual temperature difference of 20 K. This would explain the apparent discrepancy at 770 K because it is near the critical temperature for crystallization during irradiation.

The width of the diffuse diffraction rings revealed that there is at least localized atomic relaxation at temperatures below the normally observed crystallization temperature. The width of

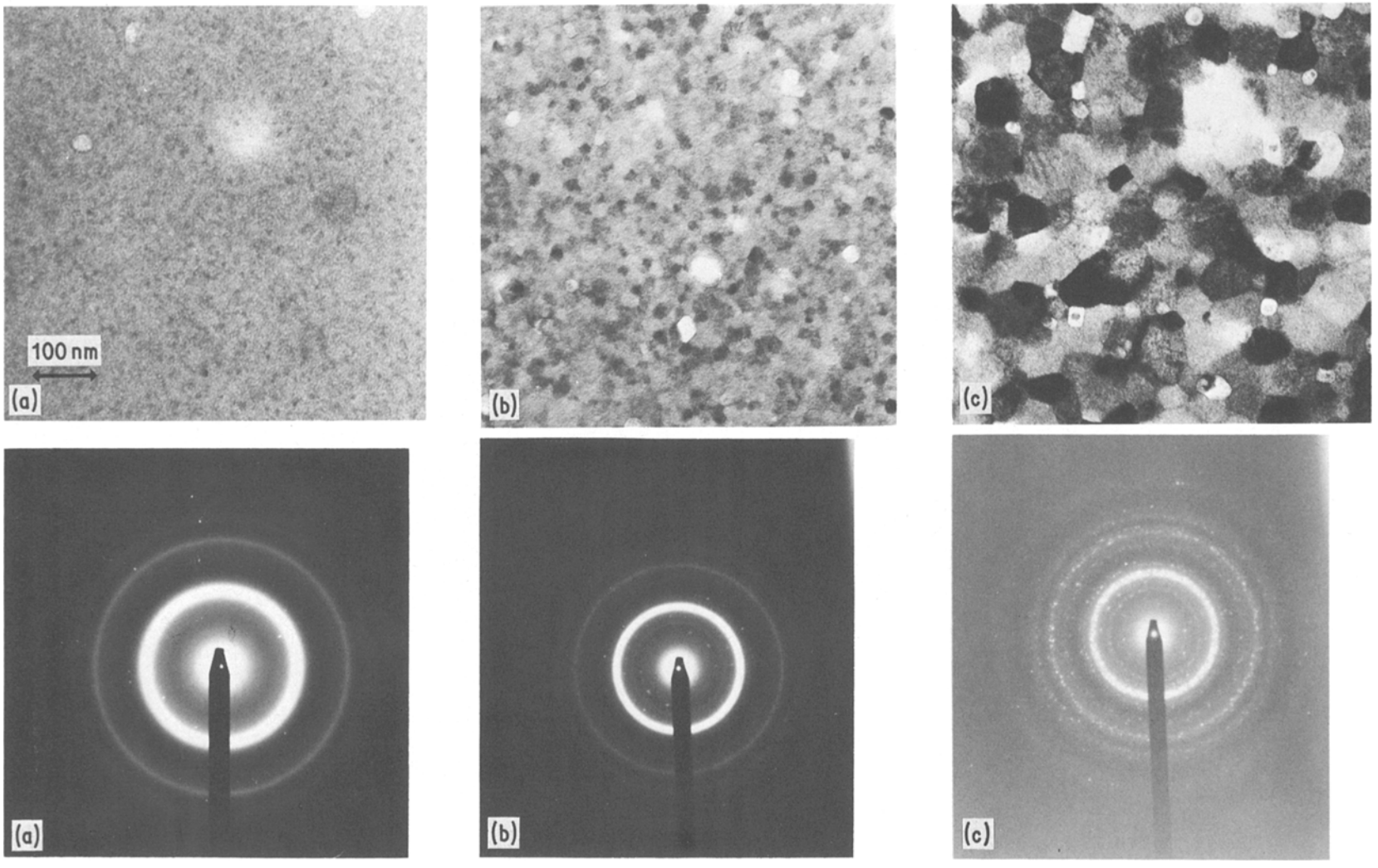

Figure 1 Amorphous MoNi irradiated with 5 MeV Ni^{2+} ions at 870 K (a) 1.5 displacements per atom, (b) 4 displacements per atom, (c) 20 displacements per atom. Bright spots in selected-area diffraction patterns are crystals of MoO_2.

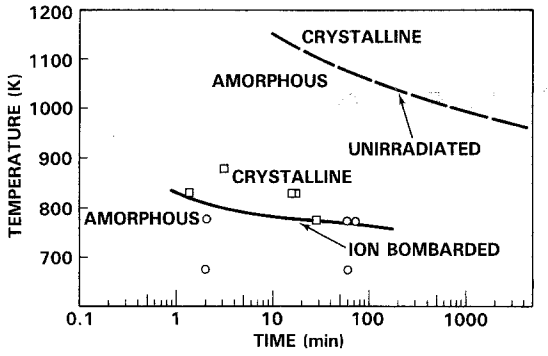

Figure 2 Time–temperature–transformation (TTT) curves for amorphous MoNi with an without ion irradiation. Unirradiated curve taken from [8]. ○ amorphous; □ crystallized.

the diffuse rings was measured with an optical densitometer, and values are shown in Table I for various annealing and irradiation conditions. A narrower width of the diffuse ring implies more structural order in the amorphous state [9]. Those MoNi alloys irradiated below 550 K or made amorphous by irradiation at 300 K showed the same width as the original sputter-deposited amorphous alloy, whereas the amorphous MoNi alloys irradiated at 770 K showed significant ordering. Thermal annealing at temperatures $\geqslant$ 870 K but before crystallization occurred also produced significant ordering.

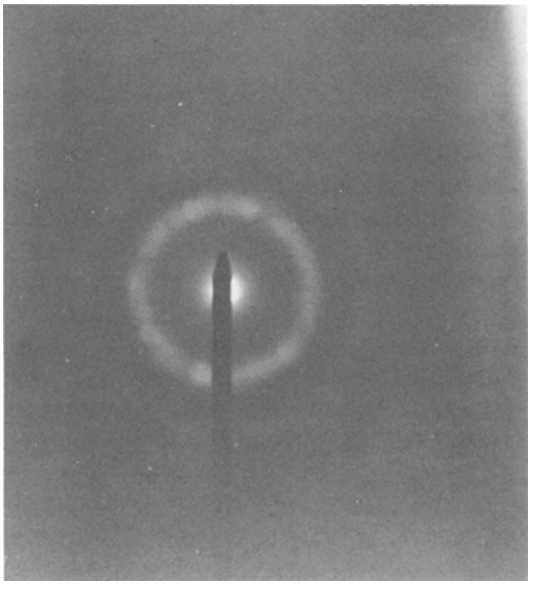

Figure 3 Microdiffraction pattern of amorphous MoNi irradiated to 1.0 displacements per atom at 870 K. Diffraction pattern taken from ~ 40 nm diameter area.

TABLE I Width of diffuse diffraction rings

Condition	Width $(4\pi \sin\theta/\lambda) \pm 0.02$
As-sputtered	0.35
Irradiated < 550 K	0.31
Made amorphous by irradiation	0.34
Irradiated 770 K	0.28
Thermal anneal 24 h 870 K	0.25
Thermal anneal 8 h 970 K	0.24
Thermal anneal 24 h 970 K	0.22

The crystallized phases after irradiation were identified as predominantly δ-phase with a small amount of MoO_2. None of the intermediate phases formed during thermal annealing were observed [8]. MoO_2, however, also forms during thermal annealing and is believed to result from oxygen contamination during sputter deposition. The ring pattern was fully consistent with the δ-phase and MoO_2. Microdiffraction from larger grains was used to obtain single-crystal patterns. Analysis was difficult due to double diffraction from twins and crystal overlap, but most of the patterns could be indexed to the δ-phase.

The grain size of the δ-phase increased with both dose and temperature (Fig. 5) and the total dose appeared to be more important than irradiation time. There is much less scatter in the data when plotted as a function of dose, as in Fig. 5, rather than time at irradiation temperature. The irradiation times were not all equivalent for equal doses as the dose rate varied.

Confirmation that these observations were due to the irradiation was possible by electrothinning completely through the bombarded zone and observing the unirradiated underlying matrix. No crystallization was observed in the underlying region except for some MoO_2 crystals. MoO_2 has been observed to form in the MoNi during annealing at temperatures $\geqslant$ 800 K, and this underlying material would have been heated to this temperature range during irradiations lasting several minutes to several hours.

3.2. Electron irradiation

Amorphous MoNi crystallized at 925 K in the electron-irradiated region after a dose of ~ 2 displacements per atom (0.25 h) (Fig. 6a). Doses up to ~ 10 displacements per atom (1.0 h) were required at 875 K before electron-induced crystallization was observable. Unirradiated regions of the foil showed no crystallization at these times and temperatures. An estimation of the crystal-

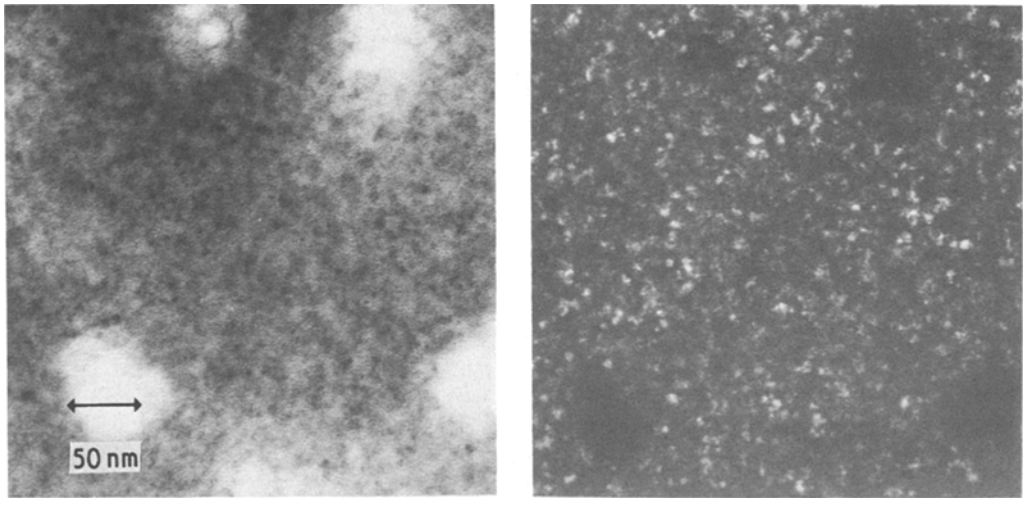

Figure 4 Bright-field and dark-field images taken from same specimen as Fig. 4. Dark-field imaged with the diffuse ring. The crystals stand out much clearer in dark-field.

lization kinetics during electron irradiation is shown in the TTT diagram in Fig. 7. The crystals initially formed in the thinnest region of the irradiated foil. At 925 K, crystallization eventually spread outside the irradiated area but only to the thinner regions (Fig. 6b). Surface nucleation is apparently significant in the crystallization of the thin foils. In bulk crystallization required many hours of thermal annealing at 975 K [8].

Investigation of the mode of crystallization was only partially successful due to apparent contamination from the HVEM environment. In a foil irradiated at 875 K, the crystals were a mixture of α-Ni and a phase tentatively identified as Mo_2C. In another foil irradiated at 925 K, a phase tentatively identified as Ni_3Mo_3 (C, O) was also observed. This phase has the structure of the ϵ-phase and was only observed in the thicker regions (the large grains in Fig. 6b). The smaller grains were a mixture of α-Ni and Mo_2C. The thin foil electron irradiated microstructure was therefore similar to the bulk material annealed at 1075 K except that there is Mo_2C in the thin foils rather than pure molybdenum as in the bulk material [8].

Amorphous Fe–Cr–Ni–W alloy crystallized at a temperature of 750 K for electron irradiation dose levels greater than 3.6 displacements per atom (0.4 h) (Fig. 8a). No evidence of crystallization was found outside the irradiated region. Continued

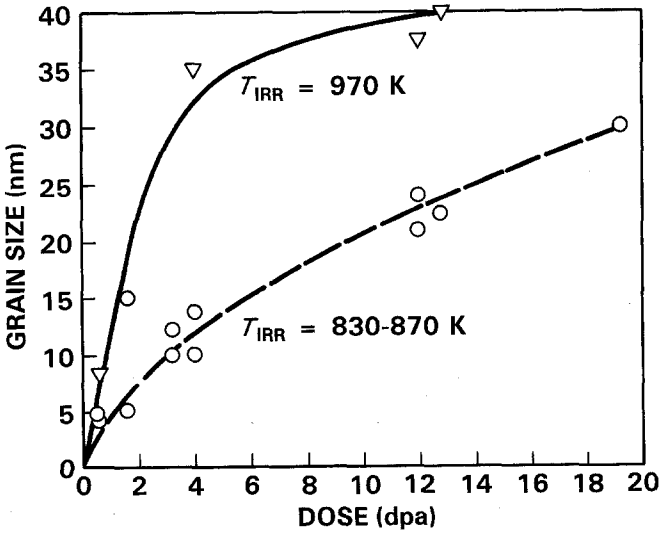

Figure 5 Grain size of δ-phase in MoNi as a function of irradiation dose.

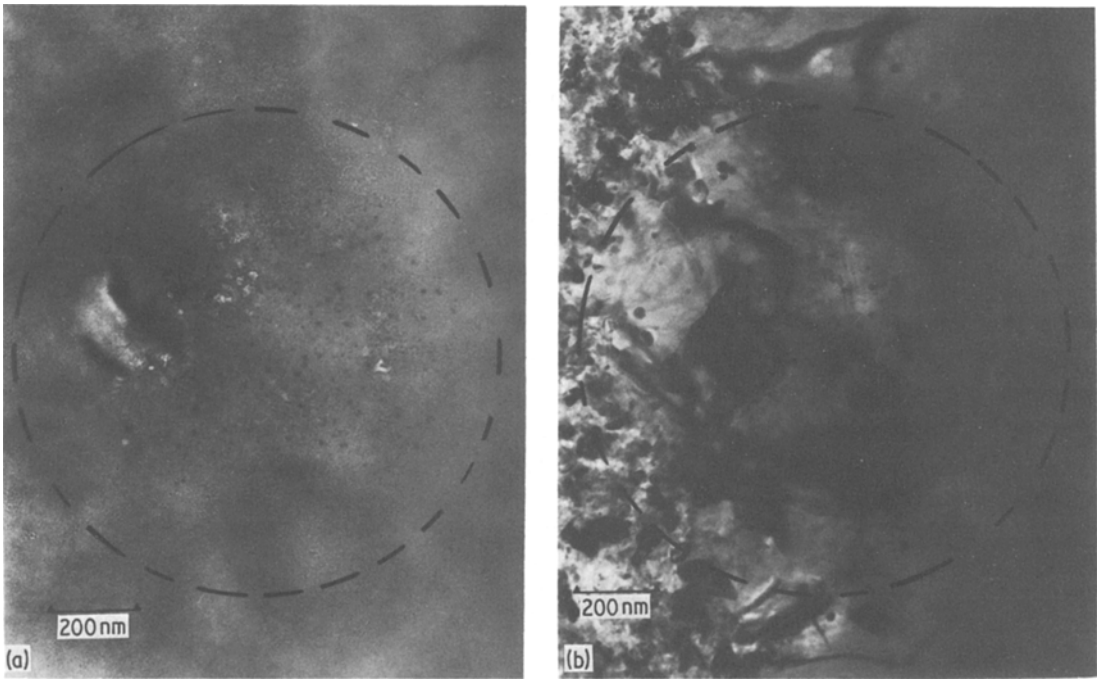

Figure 6 Amorphous MoNi irradiated with 1.5 MeV electrons at 925 K. Circle delineates irradiated area. (a) ~ 2 displacements per atom (b) ~ 4 displacements per atom.

irradiation at 750 produced more crystals but a saturation was reached after about 9 displacements per atom (1.0 h). Increasing the temperature to 810 K produced crystals beyond the edge of the irradiated zone (Fig. 8b). Continued irradiation at 810 K resulted in crystallization throughout the foil. This compares with several hours at 830 K to reach similar stages of crystallization during thermal annealing of bulk material [1]. Electron irradiation lowered T_c, but even in unirradiated regions of the thin foils, T_c was lower than that observed in bulk material during thermal annealing.

The crystals formed during irradiation were identified as bcc, α-iron solid solution with a lattice parameter of 0.278 nm. No other crystal phases were identified except an Fe_2O_3 phase in foils irradiated to 875 K. The same α-iron phase was identified within the unirradiated regions of the foil as well as in material annealed in bulk form. A primary difference between the electron irradiation and thermal annealing behaviour was the formation of a χ-phase in the remaining amorphous matrix during annealing of bulk material at temperatures $\geqslant 875$ K. Oxidation at the higher temperatures probably precluded formation of this χ-phase in the HVEM foils.

4. Discussion

The effects of irradiation on crystallization behaviour were shown to be similar for the two different alloys and the conclusions, in general, can be extended to other amorphous alloys. Both ion and

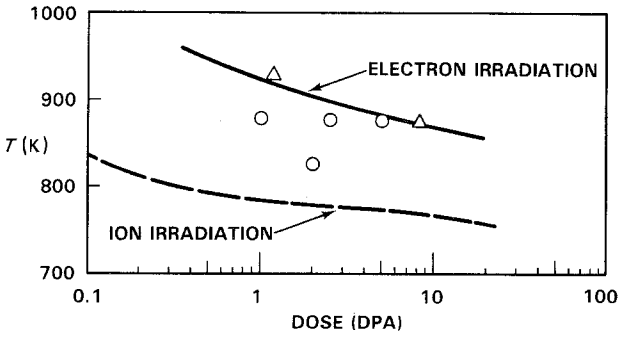

Figure 7 An estimated TTT curve for electron irradiated MoNi. The ion irradiation curve from Fig. 2 is shown for comparison. ○ amorphous; △ crystallized.

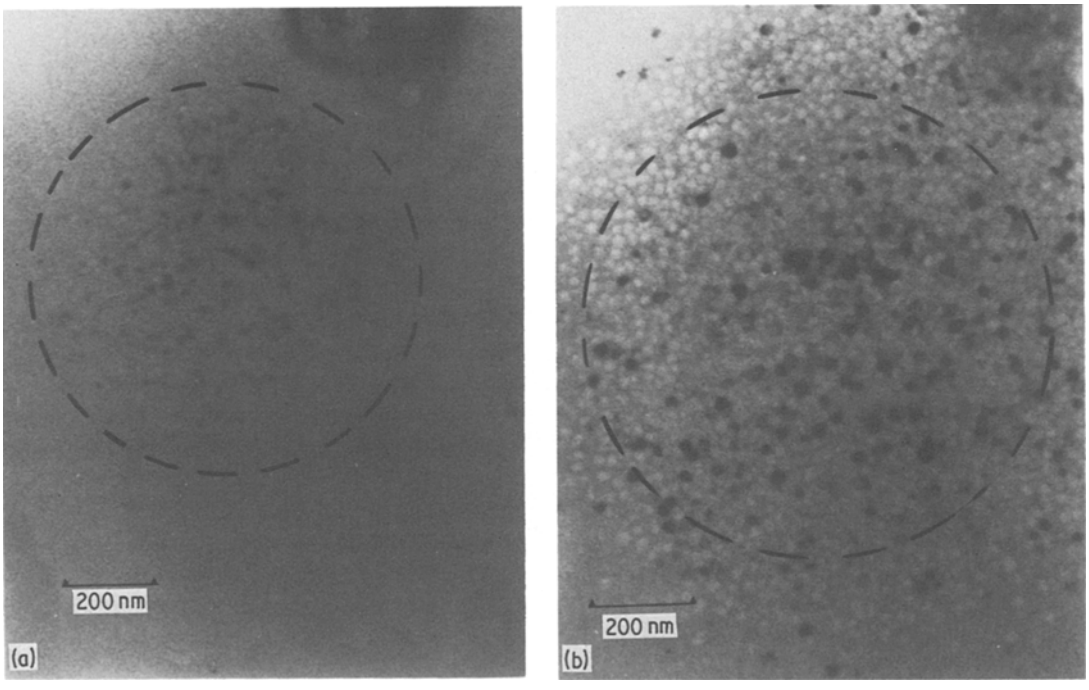

Figure 8 Amorphous Fe–Cr–Ni–W alloy electron irradiated (a) 750 K, 3.6 displacements per atom; (b) 750 K, 9 displacements per atom plus 810 K, 3 displacements per atom.

electron irradiation increased the crystallization kinetics primarily through radiation enhanced diffusion processes. Only heavy ion irradiation altered the mode of crystallization compared to electron irradiation or thermal annealing. The displacement cascades caused by the heavy ions can serve as nucleating sites for the equilibrium phase, thereby eliminating the intermediate metastable phases normally observed.

4.1. Transformation kinetics

In order for radiation-enhanced diffusion to be effective, the temperature must be sufficiently high for the atoms to have some mobility within the experimental times. The evidence showed that crystallization in these alloys during irradiation began at temperatures where short-range order occurs. The sharpening of the diffuse diffraction rings indicates that localized atomic rearrangement occurs in MoNi at annealing temperatures 100 to 200 K below T_c. Other work has shown ordering phenomena in amorphous alloys when annealed for long times below the crystallization temperature [10, 11]. This temperature range is also the same range in which diffusion measurements have been made in amorphous alloys [12]. The atoms, therefore, have an inherent mobility in this temperature regime such that the additional defects caused by irradiation increase the diffusion rate sufficiently to initiate crystallization.

If the temperature is too low, the point defects, i.e. excess free volume created by the irradiation, will be frozen in. There can be a short-range rearrangement of the amorphous configuration, but no long-range rearrangement required for crystal nucleation. Irradiating amorphous MoNi at low temperature, i.e. < 550 K, produced no changes in the diffuse diffraction rings and no observable change in microstructre. Previous irradiation studies have also shown that irradiation can produce short-range atomic order that depends on the irradiation temperature [13].

Therefore, there is a critical radiation temperature above which a crystalline phase will be stable and below which an amorphous phase will be stable. Irradiation at sufficiently low temperatures can actually render a crystalline phase completely amorphous. At high irradiation temperature, however, the crystal nuclei that are formed will be stable against any re-amorphization caused by the bombarding particle. The critical temperature will be a function of the damage rate and the inherent atomic mobilities in the crystal and amorphous phases. In MoNi, the critical temperature appears

to be in the range 670 to 770 K for the irradiation conditions used in the present study.

4.2. Crystallization mode

The unique crystallized structures observed in heavy ion bombarded materials are a result of the displacement spikes or cascades. Owing to the large energy transfer in heavy ion damage, a large number of atoms are displaced from their local atomic positions. In crystals, this is characterized by a region of high vacancy concentration from which the interstitials have escaped. Cascades in tungsten contained 200 to 500 vacancies as measured by field ion microscopy [14]. Subcascades were also identified for very high energy cascades. The large excess free volume within the cascade provides an effective nucleating site for the crystal phase. It is difficult to calculate a critical nuclei size, but the smallest crystals observed were of the order of 2 to 3 nm. This is comparable in dimension to that proposed for displacement cascades [15]. Extended-type defects, due to high energy cascades, have been proposed for ion-bombarded amorphous Pd–Si alloys [16]. Parsons and Baluffi [17] found that crystallites in amorphous germanium were directly related to cascade formation. Very low doses were used and a one-to-one correspondence was found between the observed crystals and calculated cascade concentration.

The high defect concentration and hence high short-range diffusion in the cascades will also promote the nucleation of the more complex, equilibrium crystal phases rather than the metastable phases. During thermal annealing, a mixture of pure molybdenum and either Ni_3Mo or α-Ni solid solution forms in amorphous MoNi prior to formation of the equilibrium δ-phase [8]. The amorphous Fe–Cr–Ni–W alloy also forms two phases, α-iron solid solution and χ-phase, during thermal annealing [1]. Both the δ-phase in MoNi and the χ-phase in the Fe–Cr–Ni–W alloy are complex structures with ~ 50 atoms per unit cell. Buschow and Beekmans [18] have shown that an amorphous alloy will normally crystallize by progressing through metastable phases because of the lower activation energies for the metastable transitions. Additional activation, normally supplied by higher temperatures, is required to attain the final equilibrium phase or phases. However, the very large number of atom displacements within the cascades will provide sufficient activation to directly nucleate these complex phases. The high defect concentration has the same effect as a highly localized temperature increase which promotes the equilibrium phase.

Electron irradiation, in which no cascades are formed, does not affect the type of crystallization process. The maximum energy transfer for 1.5 MeV electrons is about 200 eV. This would produce only about four displacements. The defect structure consists of a uniform distribution of isolated defects in the material. The presence of the isolated point defects will cause an increase in the long-range diffusion kinetics, but the highly enhanced short-range diffusional behaviour found in displacement cascades would not be produced by electrons. HVEM irradiation of a number of amorphous liquid-quenched alloys has generally shown some degree of acceleration of crystallization, but there have been no reports of a change in mode of crystallization [4, 5, 7].

5. Conclusion

Both electron and heavy ion irradiation lowered T_c of amorphous alloys during annealing, but heavy ion irradiation had a much stronger effect. Radiation-enhanced diffusion was postulated as being the main mechanism responsible for the acceleration of crystallization and reduced transformation temperatures. The enhancement of crystal nucleation in the displacement cascades, in addition to radiation-enhanced diffusion, can explain the stronger effect due to heavy ions. The direct transformation to the equilibrium phase by heavy ion irradiation is also a result of the high short-range diffusion rate of the atoms in the displacement cascade region.

Acknowledgements

The assistance of Homer Kissinger is gratefully acknowledged. This work was supported by the Division of Materials Service, Office of Basic Energy Sciences, US Department of Energy.

References

1. J. L. BRIMHALL, L. A. CHARLOT and H. E. KISSINGER, *J. Mater. Sci.* **17** (1982) 1149.
2. J. L. BRIMHALL, L. A. CHARLOT and R. WANG, *Scripta Metall.* **13** (1979) 217.
3. N. AZAM, L. LeNAOUR, C. RIVERA, P. GROSJEAN, P. SACOVY and J. DELAPLACE, *J. Nucl. Mat.* **83** (1979) 298.
4. M. DOI, H. KOSAKI and T. IMURA, "Rapidly Quenched Metals III", Vol. 2 (Metals Society, London, 1978) p. 372

5. M. KIRITANI, T. YOSHIIE and F. E. FUJITA, *J. Nucl. Mater.* **83** (1979) 308.
6. M. DOI, M. YOSHIDA, M. NONOYAMA, T. IMURA, T. MASUMOTO and Y. YASHIRO, *Mater. Sci. Eng.* **23** (1976) 169.
7. M. DOI and T. IMURA, *J. Mater. Sci.* **15** (1980) 2867.
8. J. L. BRIMHALL, H. E. KISSINGER and R. WANG, *ibid.* **16** (1981), 994.
9. Y. CALVAYRAC, M. HARMELIN, A. QUIVY, J. P. CHEVALIER and J. BIGOT, *Scripta Metall.* **14** (1980) 895.
10. T. EGAMI and T. ICHIGAWA, *Mater. Sci. Eng.* **32** (1978) 293.
11. T. EGAMI, *Mater. Res. Bull.* **13** (1978) 557.
12. M. KIJEK, M. AHMADZADEH, B. CANTOR and R. W. CAHN, *Scripta Metall.* **14** (1980) 1337.
13. M. NAIT SALEM and A. AUDOUARD, *ibid.* **16** (1982) 125.
14. C. Y. WEI, M. I. CURRENT and D. N. SEIDMAN, *Phil. Mag. A* **44** (1981) 459.
15. K. L. MERKLE, "Defect Production by Energetic Particle Bombardment", in "Radiation Effects in Metals", edited by N. L. Peterson and S. D. Harkness (ASM, Metals Park, 1976) pp. 58–88.
16. S. KLAUMÜNZER, G. SCHUMACHER, S. RENTZSCH and G. VOGL, *Acta. Metall.* **30** (1982) 1493.
17. J. R. PARSONS and R. W. BALUFFI, *Phys. Chem. Solids* **25** (1964), 263.
18. K. H. J. BUSCHOW and N. M. BEEKMANS, *Phys. Rev. B* **19** (1979), 3843.

Received 22 August
and accepted 13 September 1983